Ultrafast Proton Transfer Dynamics of Hydroxystilbene Photoacids

Frederick D. Lewis,*,† Louise E. Sinks,† Wilfried Weigel,‡ Meledathu C. Sajimon,† and Elizabeth M. Crompton†

Department of Chemistry, Northwestern University, Evanston, IL and Institute of Chemistry, Humboldt-University of Berlin, D-10117 Berlin, Germany

Received: November 4, 2004; In Final Form: January 15, 2005

The effects of 4-cyano and 3-cyano substituents on the spectroscopic properties and photoacidity of 3- and 4-hydroxystilbene have been investigated. In nonpolar solvents, the 3-hydroxycyanostilbenes have much longer singlet lifetimes and larger fluorescence quantum yields than do the 4-hydroxycyanostilbenes. The longer lifetimes of 3-hydroxystilbene and its cyano derivatives are attributed to a "meta effect" on the stilbene torsional barrier, similar to that previously observed for the aminostilbenes. The cyano substituent causes a marked increase in both ground state and excited-state acidity of the hydroxystilbenes in aqueous solution. The dynamics of excited-state proton transfer in methanol−water solution have been investigated by means of femtosecond time-resolved transient absorption spectroscopy. Assignment of the transient absorption spectra is facilitated by comparison to the spectra of the corresponding potassium salts of the conjugate bases and the methyl ethers, which do not undergo excited-state proton transfer. The 4-cyanohydroxystilbenes undergo excited-state proton transfer with rate constants of 5×10^{11} s^{-1}. These rate constants are comparable to the fastest that have been reported to date for a hydroxyaromatic photoacid and approach the theoretical limit for water-mediated proton transfer. The isotope effect for proton transfer in deuterated methanol−water is 1.3 ± 0.2, similar to the isotope effect for the dielectric response of water. The barrier for excited state double bond torsion of the conjugate bases is small for 4-cyano-4-hydroxystilbene but large for 4-cyano-3-hydroxystilbene. Thus the "meta effect" is observed for the singlet states of both the neutral and conjugate base.

Introduction

Electronic excitation of hydroxyaromatic molecules results in a marked increase in their acidity.[1] The isomeric naphthols and their derivatives are prototypical photoacids whose excited-state behavior have been the subject of numerous investigations. The ground- and excited-state acidities of 1-naphthol in aqueous solution are pK_a and $pK_a^* = 9.2$ and 0.4, respectively, and the singlet state undergoes deprotonation with a rate constant of $k_H = 2.5 \times 10^{10}$ s^{-1}.[2,3] Several derivatives of 1- and 2-naphthol which possess electron-withdrawing cyano- or fluoroalkanesulfonyl substituents at the 5- or 6-position have greatly enhanced excited-state acidities in water and also function as photoacids in polar, nonaqueous solvents.[4] For example, 5-cyano-1-naphthol has estimated values of $pK_a^* = -1.2$ and $k_H = 1.2 \times 10^{11}$ s^{-1} in water and undergoes excited-state proton transfer (ESPT) in alcohol solvents.[5] The cyanonaphthols have been referred to as "super" photoacids.

Essentially all measurements of photoacid pK_a^* and k_H values are based on analysis of the fluorescence properties of the neutral hydroxyaromatic, ROH, and its conjugate base RO^-. The former property is most readily obtained using the Förster equation, eq 1,

$$pK_a^* = pK_a - (h\nu_1 - h\nu_2)/2.3RT \qquad (1)$$

where $h\nu_1$ and $h\nu_2$ are the zero−zero transitions for the acid and its conjugate base, and pK_a is the ground-state acidity constant.[6,7] Values of k_H are derived from the fluorescence decay of ROH* or the rise of the fluorescence of RO^-*.[8] The reliance on fluorescence precludes the study either of super photoacids for which proton transfer is so fast that ROH* fluorescence is too weak to permit accurate decay measurements or of photoacids with nonfluorescent conjugate bases. Transient absorption spectroscopy with femtosecond (fs) time resolution has been employed to study the dynamics of ESPT from the photoacid 8-hydroxypyrene-1,3,6-trisulfonate to acetate ion in water[9,10] and from 6-hydroxyquinoline and camptothecins containing the 6-hydroxyquinoline subunit to water.[11,12]

We recently reported the results of an investigation of the excited-state behavior of 3- and 4-hydroxystilbene (3SOH and 4SOH, Chart 1) in several solvents.[13,14] 3SOH was found to behave as a strong photoacid, displaying fluorescence from both 3SOH* and $3SO^-$* in aqueous solution with a Förster $pK_a^* \sim 0.1$. However, 4SOH exhibits fluorescence from 4SOH*, but not from $4SO^-$* in aqueous solution. This substituent positional effect was attributed to a lower barrier for C=C torsion in 4SOH* vs 3SOH*, which results in a very short singlet lifetime for 4SOH*. Attempts to measure the fluorescence decay time of 4SOH* with an apparatus having a 50 ps instrument function were unsuccessful.

We report here the use of fs transient absorption spectroscopy to investigate the dynamics of ESPT from the 4-cyanohydroxystilbenes 43SNOH and 44SNOH and their 3-cyano isomers 33SNOH and 34SNOH in methanol−water (MW) solution. The transient spectra of 3SOH and 4SOH have also been investigated for the first time. The use of MW is necessitated by the low solubility of the hydroxystilbenes in water. The transient spectra of methoxy derivative 44SNOMe (Chart 1) and the conjugate

* Corresponding author. E-mail: lewis@chem.northwestern.edu.
† Northwestern University.
‡ Humboldt-University of Berlin.

10.1021/jp044942s CCC: $30.25
Published on Web 02/26/2005

CHART 1

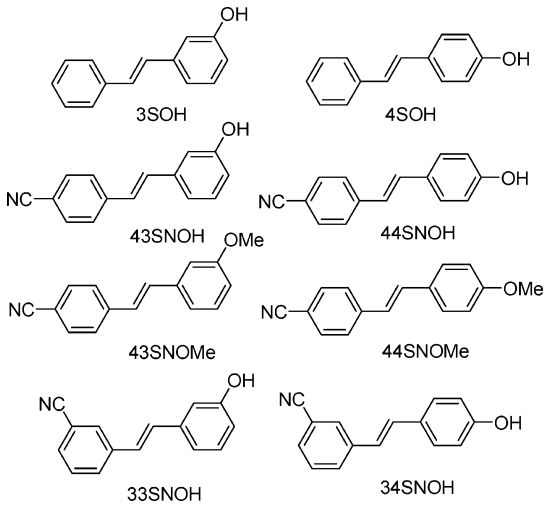

base $44SNO^-$ provide reference analogues which are incapable of undergoing ESPT. The 4-cyanohydroxystilbenes have rate constants for ESPT of $k_H \sim 5 \times 10^{11}$ s^{-1}, comparable to the fastest that have been observed to date for a photoacid.[11] Lower rate constants are observed for 33SNOH and 3SOH, whereas the occurrence of ESPT cannot be detected by transient absorption spectroscopy for 34SNOH and 4SOH. The effects of substituent position upon singlet lifetimes, ESPT dynamics, and isomerization efficiency are discussed.

Experimental Section

Materials. The *trans*-cyanomethoxystilbenes 43SNOMe and 44SNOMe were synthesized by the Wittig reaction between 4-cyanobenzyl triphenylphosphonium bromide with the appropriate anisaldehyde (meta or para).[15] Yields were about 50%. Products were characterized by NMR and GC/MS.

4-Cyano-3′-methoxystilbene (43SNOMe): ^{1}H NMR ($CDCl_3$, 400 MHz) δ 3.86 (s, 3H), 6.84−6.90 (dd, 1H), 7.02−7.11 (m, 2H), 7.11−7.15 (d, 1H), 7.16−7.22 (d, 1H), 7.28−7.34 (t, 1H), 7.55−7.61 (d, 2H), 7.62−7.67 (d, 2H); MS *m*/e: $M^+ = 235$.

4-Cyano-4′-methoxystilbene (44SNOMe): ^{1}H NMR ($CDCl_3$, 400 MHz) δ 3.84 (s, 3H), 6.88−6.99 (m, 3H), 7.13−7.20 (d, 1H), 7.45−7.50 (d, 2H), 7.53−7.58 (d, 2H), 7.58−7.65 (d, 2H); MS *m*/e: $M^+ = 235$.

The cyanomethoxystilbenes were converted to the corresponding cyano-hydroxystilbenes by the procedure of McOmie et al.[16] Yields were 30−60%. Products were characterized by NMR and GC/MS.

4-Cyano-3′-hydroxystilbene (43SNOH): ^{1}H NMR ($CDCl_3$, 400 MHz) δ 4.98 (s, 1H), 6.76−6.83 (dd, 1H), 7.01 (br s, 1H), 7.03−7.09 (d, 1H), 7.09−7.12 (d, 1H), 7.13−7.19 (d, 1H), 7.22−7.29 (t, 1H), 7.54−7.60 (d, 2H), 7.61−7.67 (d, 2H); MS *m*/e: $M^+ = 221$.

4-Cyano-4′-hydroxystilbene (44SNOH): ^{1}H NMR ($CDCl_3$, 400 MHz) δ 5.12 (s, 1H), 6.83−6.88 (d, 2H), 6.90−6.98 (d, 1H), 7.10−7.19 (d, 1H), 7.40−7.47 (d, 2H), 7.52−7.58 (d, 2H), 7.58−7.65 (d, 2H); MS *m*/e: $M^+ = 221$.

3-Cyano-3′-hydroxystilbene (33SNOH): ^{1}H NMR ($CDCl_3$, 400 MHz) δ 4.86 (s, 1H), 6.75−6.81 (dd, 1H), 6.97−7.06 (m, 2H), 7.07−7.14 (m, 2H), 7.22−7.30 (t, 1H), 7.43−7.49 (t, 1H), 7.51−7.56 (d, 1H), 7.67−7.74 (d, 1H), 7.77 (s, 1H); MS *m*/e: $M^+ = 221$.

3-Cyano-4′-hydroxystilbene (34SNOH): ^{1}H NMR ($CDCl_3$, 400 MHz) δ 5.13 (s, 1H), 6.82−6.88 (d, 2H), 6.88−6.97 (d, 1H), 7.06−7.14 (d, 1H), 7.38−7.46 (m, 3H), 7.48−7.52 (d, 1H), 7.66−7.71 (d, 1H), 7.75 (s, 1H); MS *m*/e: $M^+ = 221$.

Methods. Ground and excited-state dipole moments were estimated and pK_a values were determined as previously described.[14] UV−vis spectra were recorded on a Hewlett-Packard 8452A or 8453 diode array spectrophotometer using a 1 cm path length quartz cell. Fluorescence spectra were measured on a SPEX FluoroMax fluorometer. Fluorescence quantum yields and ns decays were measured as previously described.[14] Subnanosecond decays were obtained with a Ti:sapphire-pumped system with single-photon counting detection having an instrument response function of 50 ps.[17] All spectroscopic measurements were performed on solutions that were purged with dry N_2 for at least 25 min. ZINDO calculations were performed using the ZINDO algorithm as implemented in CAChe version 4.4.[18]

Transient absorption spectroscopy was carried out using a femtosecond transient absorption system with an optical parametric amplifier (OPA), as described elsewhere.[19] The UV light was generated by tuning the OPA to 640 nm, and the resulting light was sent down the track, and was then focused into a 1 mm BBO crystal ($\theta = 40.5°$, $\varphi = 0°$) with a 100 mm f.l. lens. The light was recollimated with a 200 mm f.l. lens, and then focused into the sample using a 200 mm f.l. lens. The residual 640 nm OPA light was filtered from the UV light, and between 0.3 and 0.5 μJ per pulse of 320 nm light was produced at the sample. The resulting pump light was vertically polarized, and the white light probe (generated with CaF_2) was set to the magic angle with a calcite polarizer. The probe beam was chopped according to the scheme in Lukas et al.[20] Detection was accomplished with a CCD array detector (Ocean Optics PC2000) for simultaneous collection of spectral and kinetic data.[21] The total instrument response function for the pump−probe experiments was 130 fs. Five seconds of averaging were typically needed to obtain the transient spectrum at a given delay time. Cuvettes with a 2 mm path length were used, and the samples were irradiated with 0.3−0.5 μJ per pulse focused to a 200 μm spot. The sample was stirred with a wire stirrer to prevent thermal lensing and sample degradation. Absorption spectra were recorded before and after laser excitation. Kinetic analyses were performed at several wavelengths using a Levenberg−Marquardt nonlinear least-squares fit to a general sum-of-exponentials function with an added Gaussian to account for the finite instrument response.

Results and Discussion

Absorption and Emission Spectra. The absorption and fluorescence spectra of 43SNOH and 44SNOH in MW and in 50% methanol/0.1 M KOH (MW−KOH) are shown in Figure 1. The appearance of the absorption spectra in MW and MW−KOH are similar to those previously reported for 3SOH and 4SOH in water and aqueous base.[13,14] Absorption spectra of both 43- and 44-SNOH in 50% v/v methanol/water (MW) display a strong long-wavelength absorption band. The absorption spectrum of 44SNOH in MW−KOH also displays a red-shifted band. The absorption spectrum of 43SNOH in MW−KOH is more complex (Figure 1a), consisting of a long-wavelength shoulder and a strong band at shorter wavelength. The absorption spectra of 33- and 34SNOH are similar to those of the 4-cyano isomers. Absorption maxima in several solvents are reported in Table 1.

The long-wavelength absorption bands of the cyanohydroxystilbenes are assigned to essentially pure π,π^* HOMO→LUMO transitions on the basis of semiempirical ZINDO calcula-

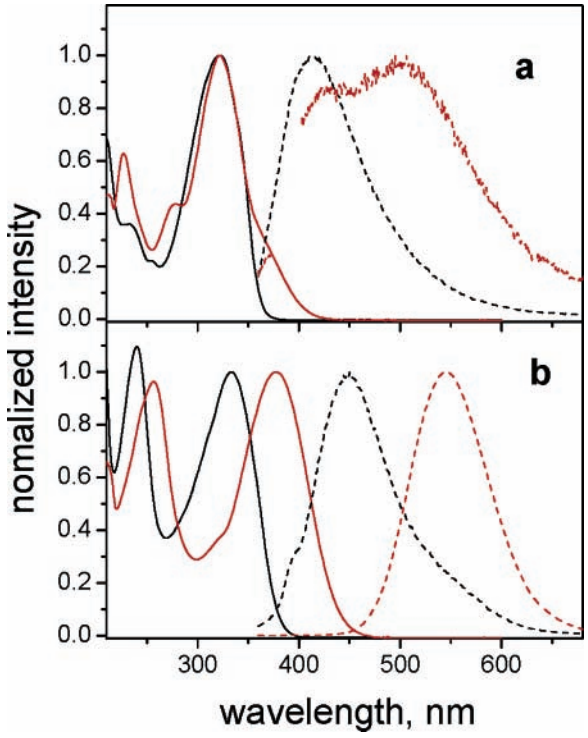

Figure 1. Normalized absorption (solid lines) and fluorescence spectra (broken lines) of (a) 43SNOH and (b) 44SNOH in MW (black lines) and MW−KOH (red lines).

TABLE 1: Spectral Data for 4′-Cyanohydroxystilbenes

	solvent[a]	λ_{abs}, nm	λ_{fl}, nm	Φ_{fl}[b]	τ_s, ns[c]
43SNOH	THF	320	401	0.40	1.3
	MeOH	320	417	0.22	
	MW	322	401	0.02	
	MW−KOH	322,373	420,501	<0.01	
	H_2O	321	415		
44SNOH	THF	343	415	0.02	<0.05
	MeOH	337	435	0.03	<0.05, 0.014[d]
	MW	334	452	0.04	
	MW−KOH	379	545	0.01	0.23
	H_2O	330	455		
43SNOMe	THF	322	391	0.25	0.42
	MeOH	320	404		
44SNOMe	THF	338	412	0.02	<0.05
	MeOH	338	434		
33SNOH	THF	298	361	0.53	2.6
	MeOH	295	394	0.76	
	MW	294	395	0.03	
	H_2O	293	398		
34SNOH	THF	320	402	0.03	0.096
	MeOH	318	426	0.03	0.012[d]
	MW	320	406	0.02	
	H_2O	320	431		

[a] MW = 50% v/v methanol−water. MW−KOH = 50% methanol, 50% 0.1 M aqueous KOH. [b] Fluorescence quantum yields determined on deoxygenated solutions at room temperature. [c] Fluorescence decay times determined on deoxygenated solutions at room temperature. Values of <0.05 indicate decay times too short for measurement with a laser-based lifetime apparatus having an instrument response function of 50 picoseconds. [d] Values determined by transient absorption spectroscopy.

tions.[22,23] The HOMO is ethylene-localized and the LUMO is cyanostyrene-localized, as shown in Figure 2a for 44SNOH, providing a moderate degree of charge transfer to this transition. The red-shifted long-wavelength band of $44SNO^-$ in MW−KOH is also assigned to a HOMO→LUMO transition (Figure 2b). In this case the HOMO is phenoxide-localized and the LUMO benzonitrile-localized, resulting in a high degree of charge transfer. The absorption band of $43SNO^-$ is split into two bands of different intensity as a consequence of symmetry breaking by the meta substituent.[24] ZINDO calculations for the four lowest singlet states of the cyanohydroxystilbenes are reported as Supporting Information. Formal charges on oxygen obtained from ZINDO calculations for the ground states of the hydroxystilbenes and their conjugate bases are reported in Table 2.

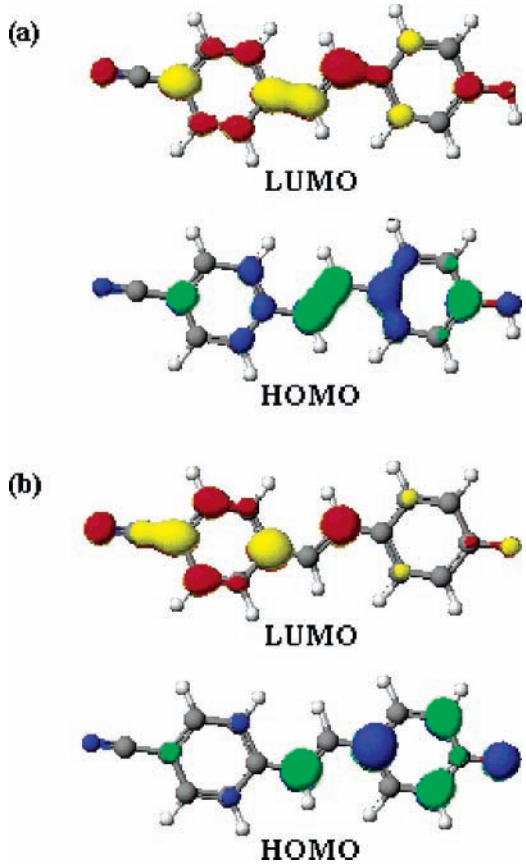

Figure 2. ZINDO frontier orbitals (HOMO and LUMO) for (a) 44SNOH and (b) $44SNO^-$.

TABLE 2: Formal Charges, Dipole Moments, and Acidities of the Ground and Excited States

	$-q_o(ROH)$[a]	$-q_o(RO^-)$[a]	μ_g, D[b]	μ_e[c]	pK_a[d]	pK_a*[e]
3SOH[f]	0.485	0.882	1.83	9.09	10.1	0.1
4SOH[f]	0.484	0.785	1.88	6.56	9.3	2.0
43SNOH	0.482	0.774	6.68	11.3 (19.0)	9.1	*g*
44SNOH	0.482	0.768	5.20	10.6 (19.3)	8.5	0.6
33SNOH	0.483	0.818	6.85	7.6 (17.0)	9.1	*g*
34SNOH	0.482	0.774	3.37	15.0 (18.3)	8.6	*g*

[a] Formal charges on oxygen obtained from ZINDO calculations for the hydroxystilbenes (ROH) and their conjugate bases (RO^-). [b] Ground-state dipole moment calculated in CAChe using PM3 calculated geometries. [c] Excited-state dipole moments calculated from solvatochromic data using the method of Liptay. Values for the FC and CT (data in parentheses) excited states. [d] Experimental values in water obtained spectrophotometrically. [e] Excited-state values in water obtained using the Förster equation. [f] Data from ref 12. [g] Fluorescence too weak to permit determination.

The fluorescence spectra of the cyanohydroxystilbenes in cyclohexane solution display vibronic structure (data not shown), similar to that of *trans*-stilbene and the isomeric aminostilbenes.[24] In THF and more polar solvents, they appear as a broad, structureless band, as shown in Figure 1 for 43- and 44SNOH in MW solution. In MW−KOH solution, the fluorescence spectra are shifted to longer wavelength and are

SCHEME 1

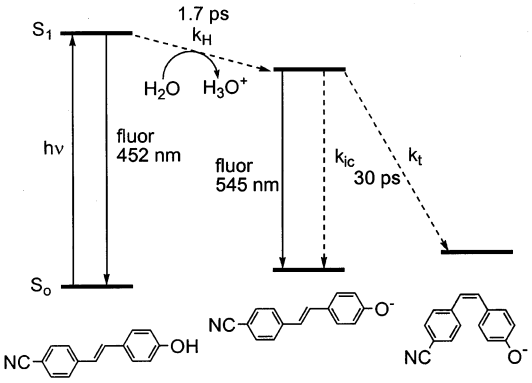

attributed to the conjugate bases 43SNO$^-$ and 44SNO$^-$. A weak long-wavelength shoulder attributed to the conjugate base 44SNO$^-$ is observed in the fluorescence spectrum of 44SNOH in MW, but not in the spectrum of 43SNOH. Weak conjugate base fluorescence may result from either inefficient formation of SNO$^-$* or a low fluorescence quantum yield (Scheme 1). Absorption and fluorescence spectral data for the cyanohydroxystilbenes and their methoxy analogues in several solvents are summarized in Table 1. The spectra of the alcohols and their methoxy analogues are similar both in band shape and absorption maxima and display only modest solvent-induced shifts (except in the case of 44SNOH in MW−KOH). Spectra of the alcohols in water and aqueous base are similar to those in MW and MW−KOH.

Fluorescence quantum yields (Φ_f) and singlet lifetimes (τ_s) for the cyanohydroxystilbenes and their methoxy analogues in several solvents are reported in Table 1. The meta-substituted isomers 43SNOH, 43SNOMe, and 33SNOH have larger values of Φ_f and longer values of τ_s than do the para-hydroxy-substituted isomers in THF or MeOH solution. This trend has been previously noted for 3SOH and 4SOH as well as for the corresponding aminostilbenes.[13,14,24] The longer lifetimes of meta- vs para-substituted stilbenes possessing strong, electron-donating substituents is attributed to the ability of the meta substituent to selectively stabilize the planar singlet vs twisted singlet, resulting in an increased barrier for C=C torsion and an increased singlet lifetime.

Dipole Moments and Ground-State Acidities. Ground and excited-state dipole moments and acidities for the cyanohydroxystilbenes are summarized in Table 2 along with published data for the hydroxystilbenes.[14] Ground-state dipole moments were calculated in CAChe using PM3 optimized geometries.[18] The increase in μ_g upon addition of a 4-cyano substituent is similar to that previously reported for the aminostilbenes.[25] The dipole moments of the Franck−Condon (μ_{FC}) and charge-transfer excited states (μ_{CT}) were calculated from the solvent dependence of the absorption and fluorescence maxima, respectively, using standard methods, as previously described for the aminostilbenes (see Supporting Information).[25] The resulting values are similar to those reported for the aminostilbenes and are indicative of a moderately polar LE state, in accord with the ZINDO description of the vertical singlet state (Figure 2a), and a highly polar CT state.[22] More accurate analysis of specific solvent effects on the fluorescence spectra of photoacids is possible using a Kamlet−Taft analysis.[14,26] However, the values reported in Table 2 suffice to establish the enhanced CT character of the cyanohydroxystilbenes when compared to the hydroxystilbenes.

Ground state acidities were determined titrametrically in aqueous solution. The introduction of a cyano substituent results in an increase in acidity of ca. 1 pK_a unit for both the cyanohydroxystilbenes vs 3SOH and 4SOH, respectively (Table 2). This increase in acidity is smaller than that for 6-cyano-2-naphthol vs 2-naphthol (pK_a = 10.5 and 8.8, respectively).[27] The excited-state acidity of 44SNOH in aqueous solution was estimated using the Förster equation (eq 1). The value of pK_a* for 44SNOH* indicates an increase in excited-state acidity by 1.4 pK_a units upon introduction of the 4-cyano substituent. This increase is also smaller than that for 6-cyano-2-naphthol vs 2-naphthol (pK_a* = 0.2 and 2.8, respectively).[8] The very weak fluorescence of the other conjugate bases precludes determination of their pK_a* values by either a Förster cycle or more accurate methods such as fluorescence titration[7] and singular value decomposition with self-modeling.[13]

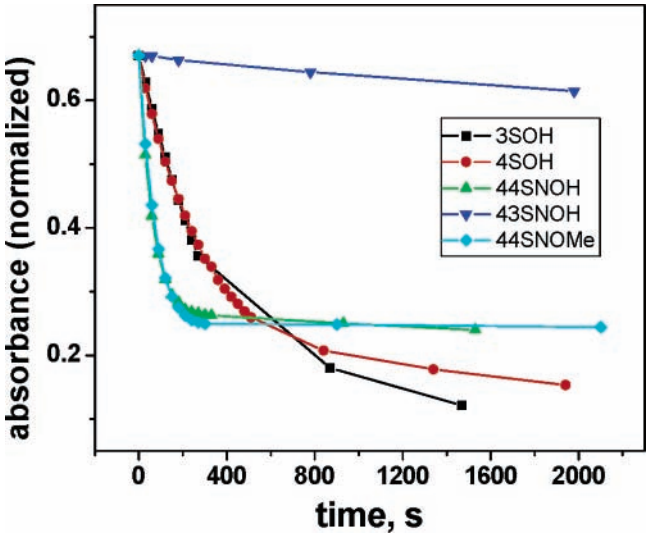

Figure 3. Time-dependent absorbance of the hydroxystilbenes in MW solution monitored at their absorption maxima with monochromatic irradiation at their absorption maxima in MW solution.

Irradiation in Methanol−Water Solution. Murohoshi et al.[28] have reported that the trans isomers of 3SOH and 4SOH have high quantum yields for conversion to a mixture of the cis isomer and stilbene-water adduct in 1:1 MeCN/H_2O (Φ = 0.36 and 0.49, respectively). We have investigated the steady-state irradiation of 3- and 4SOH, 44- and 43SNOH, and 44SNOMe in MW solution. The time-dependent changes in long-wavelength absorbance is shown in Figure 3. Both 3- and 4SOH display an initial rapid decrease in absorbance attributed, by analogy to the results of Murohoski et al.,[28] to trans−cis isomerization and a slower bleaching attributed to solvent addition and phenanthrene formation. 43SNOH is relatively stable upon irradiation, indicative of inefficient trans-cis isomerization. In contrast 44SNOH and 44SNOMe undergo rapid reaction to a constant absorbance, attributed to the formation of a steady-state mixtures of trans and cis isomers, which do not undergo further reaction.

Transient Absorption Spectroscopy of 44SNOH, 44SNO$^-$, and 44SNOMe. Transient absorption spectra were obtained using a Ti:sapphire based laser system with a CCD array detector for simultaneous collection of spectral and kinetic data.[21] The total instrument response function for the pump−probe experiments is 130 fs. Samples were stirred and their absorption spectra recorded before and after measurement of their transient spectra. We are confident that the transients observed can be attributed to the singlet states of the trans isomers and their conjugate bases rather than their nonfluorescent cis isomers or methanol adducts. Assignment of the transient spectra of 44SNOH and the other hydroxystilbenes is

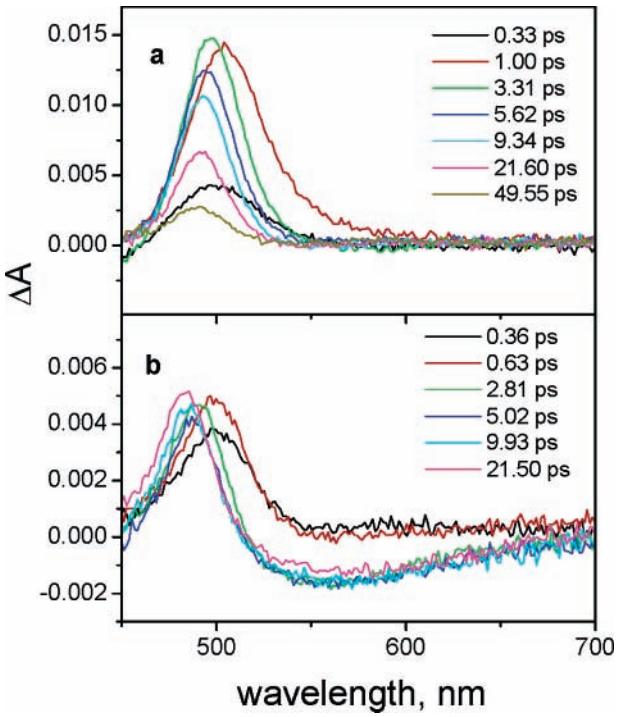

Figure 4. Transient absorption spectra for (a) 44SNOMe and (b) 44SNO$^-$ in MW solution.

complicated by the overlapping absorption bands of the photoacid and its conjugate base. However, comparison of their transient spectra with those for 44SNOMe and 44SNO$^-$, which cannot undergo ESPT permits assignment of the more complex spectra of 44SNOH. Our assignments of the transient absorption spectra of the hydroxystilbenes are similar to those reported by Cohen et al.[10] for proton transfer between the photoacid 8-hydroxypyrene-1,3,6-trisulfonate and the base acetate ion in water and to those reported by Poizat et al.[11] for proton transfer from 6-hydroxyquinoline to water.

The transient spectra of 44SNOMe display initial formation of a band with a maximum near 500 nm within ca. 1 ps, followed by a blue shift in the band maximum to 480 nm within the next several ps (Figure 4a), accompanied by band-narrowing. Single-wavelength kinetics determined at 10 nm intervals across the band establish that the 500 nm band has a rise time of 0.26 ps, slightly longer than the instrument response function, and that band-narrowing occurs with a decay time of 2.1 ps. Finally, the decay of the 480 nm band is dominated by a 33 ps decay component. This short decay time is consistent with the upper bound of 50 ps for the lifetime of 44SNOMe in THF estimated from attempted fluorescence decay measurements (Table 1).

Band narrowing of the initially formed transient is attributed to vibrational relaxation of the stilbene FC excited state. Stilbene singlet excited states are known to have more planar energy minima than the corresponding ground states.[29] Vibrational relaxation of stilbene FC singlet states has been investigated by means of a number of time-resolved methods, including transient absorption, Raman, anti-Stokes Raman scattering spectroscopy, and time-resolved emission.[30−32] These studies provide relaxation times of ca. 2 ps, similar to the band narrowing for 44SNOMe (Table 3). It is interesting to note that neither *trans*-stilbene[30] nor its 4,4-dicarboxamide derivative[33] display shifts in their transient absorption band maxima upon vibrational relaxation in nonaqueous solution. However, the fluorescence of 4-(dimethylamino)-4′-cyanostilbene and other push−pull substituted stilbenes undergo a blue shift attributed to relaxation from the FC to CT singlet state with a decay time

TABLE 3: Dynamics of Singlet State Formation, Relaxation, and Decay and Conjugate Base Formation and Decay[a]

	τ_{rs} (500)[b]	τ_{vr} (530)[c]	τ_{ds} (480)[d]	τ_{rcb} (420)[e]	τ_{dcb} (420)[f]
3SOH	0.15	2.3	29	37	490
4SOH	0.16	2.1	17		
43SNOH	0.14		1.1[g]	2.8	25
44SNOH	0.16		1.7[g]	1.7	30, 27[h]
4SNOD[i]	0.16		1.9[g]	2.1	36, 21[h]
44SNO$^-$	0.16	1.8	240, 340[h]		
43SNOMe	0.26	2.4	246		
44SNOMe	0.22	2.1	33		
33SNOH		2.6		4.6	19
34SNOH		1.8	12		

[a] Kinetics in picoseconds determined at wavelengths indicated in parentheses (except as noted) in MW solution (except as noted). [b] Rise time for 500 nm transient. [c] Vibrational relaxation time. [d] Decay of the singlet state. [e] Rise time for the conjugate base. [f] Decay of the conjugate base. [g] Decay times determined at 510 nm. [h] Rise time for the 540 nm emissive band. [i] Data for MeOD/D_2O.

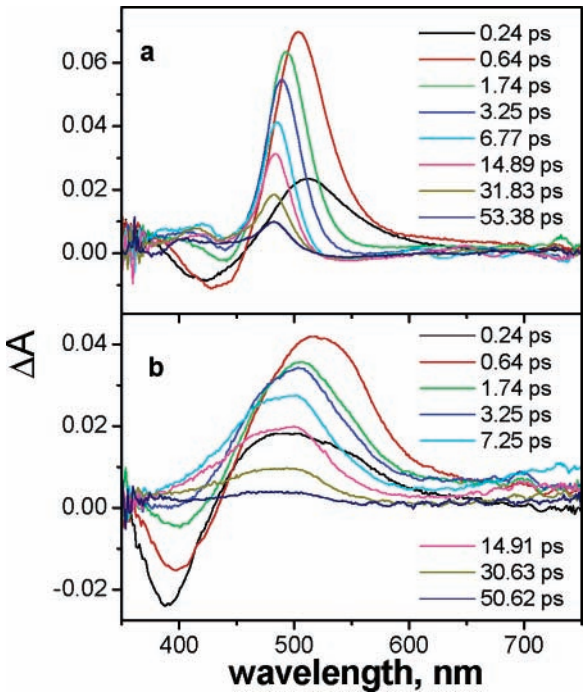

Figure 5. Transient absorption spectra for (a) 44SNOH and (b) 43SNOH in MW solution.

of ca. 5−7 ps in ethanol solution.[32,34] It is likely that relaxation from the initially formed FC singlet state to the CT singlet state of the cyanohydroxystilbenes is responsible for the band shift observed in MW solution.

The transient spectra of 44SNOH in MW−KOH shown in Figure 4b are assigned to the formation and decay of the singlet state of the conjugate base 44SNO$^-$*. The 500 nm transient is formed with an instrument-limited rise time and relaxes to the 485 nm transient with a decay time of 2.9 ps, values similar to that for 44SNOMe. In addition, there is a broad emissive band centered near 550 nm, which forms rapidly (ca. 1 ps) and decays with a rise time similar to the decay time of the 480 nm band (Table 3). These long-lived transients are assigned to the absorption and fluorescence of 44SNO$^-$* and have lifetimes similar to the fluorescence decay of 44SNOH in MW−KOH (Table 1).

We turn next to the transient spectra of 44SNOH (Figure 5a). The most prominent feature of its spectra is the formation of the 500 nm transient with an instrument-limited rise time, followed by band narrowing with a shift to 480 nm, with a time

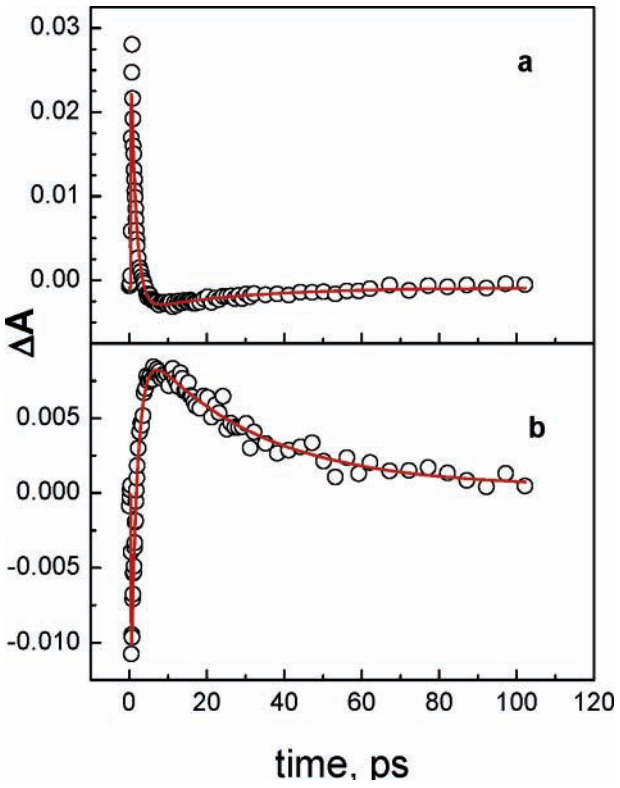

Figure 6. Transient decay of 44SNOH in MW solution monitored at (a) 541 and (b) 421 nm.

constant of 1.7 ps obtained from the 510 nm decay. Since the singlet states of both 44SNOMe and $44SNO^-$ have transient absorption bands near 480 nm, this band cannot be assigned with certainty to either the singlet or its conjugate base. The band shift is accompanied by the appearance of a weak emissive band near 540 nm, assigned to the fluorescence of $44SNO^{-}$*. The transient kinetics for the formation and decay of this emissive band are shown in Figure 6a. The decay and rise are fit to 1.4 and 27 ps, respectively (Table 3).

In addition to these long-wavelength components, an emissive component with a minimum at 430 nm is formed within 1 ps. This component is assigned to the fluorescence of 44SNOH*, which has a steady-state fluorescence maximum at 435 nm in methanol solution (Table 1). This emissive band is replaced by a 420 nm absorption band, which has a rise time of 1.7 ps (Figure 6b). The similarity of this rise time to the 1.4 ps 510 nm decay and the appearance of the $44SNO^{-}$* fluorescence band permit assignment of the 420 and 480 nm absorption bands to the absorption spectrum of $44SNO^{-}$*. Both the 420 nm absorption and 540 nm emission bands have decay times of ca. 30 ps. The rise and decay times assigned to $44SNO^{-}$* formed upon irradiation of singlet 44SNOH in MW are summarized in Table 3.

The effects of solvent deuteration and solvent composition on the transient absorption spectra of 44SNOH have been briefly investigated. The transient absorption spectra of 44SNOH in CH_3OD/D_2O (MW-*d*) are similar to those in MW. Decay times for the singlet and its conjugate base in MW-*d* are reported in Table 2 and are discussed later. Both in pure methanol and 9:1 methanol−water (v/v) the transient spectra for 44SNOH are similar to those for 44SNOMe in 1:1 MW (Figure 4a). A 510 nm absorption band is formed with an instrument-limited rise time and undergoes a blue shift to 480 nm with a decay time of ca. 2 ps, attributed to vibrational cooling. The 480 band has decay times of 17 and 14 ps in 9:1 methanol/water and pure methanol, respectively, attributed to nonradiative decay (via C═C torsion) of 44SNOH*, which is weakly fluorescent in methanol (Table 1). Thus we conclude that 44SNOH* fails to undergo ESPT to an appreciable extent in either methanol or 9:1 MW.

Transient Absorption Spectra of 43SNOH, 33SNOH, and 34SNOH. The transient absorption spectra of 43SNOH in MW shown in Figure 5b differ from those of 44SNOH in displaying a broader absorption band, no long-wavelength emissive component, and a stronger short-wavelength emissive band. The absence of long-wavelength emission is consistent with the fluorescence spectra of 43SNOH* in MW which shows no component of $43SNO^-$ emission (Figure 1a). The broader 480 nm band for $43SNO^{-}$* vs $44SNO^{-}$* may be a consequence of the presence of two rotational isomers for 43SNOH and its conjugate base or simply the loss of symmetry in meta- vs para-substituted stilbenes. The 2.8 ps rise time of the 420 nm shoulder of the broad absorption band can be assigned to the formation of $43SNO^{-}$*, and the 25 ps decay time can be assigned to the disappearance of $43SNO^{-}$*. The dynamics of the formation and decay of 43SNOH* and $43SNO^{-}$* are summarized in Table 3.

The transient spectra of 43SNOMe (not shown) are somewhat broader than those of 44SNOMe (Figure 4a), but have similar rise and decay times for the formation and narrowing of the 500 nm band (Table 2). The 250 ps decay time for the 480 nm transient is similar to the fluorescence decay time of 43SNOMe* in THF solution (Table 1) and is assigned to decay of the singlet state.

The transient absorption spectra of 33SNOH (provided as Supporting Information) closely resemble those of 43SNOH (Figure 5b). The rise time for formation of $33SNO^{-}$* is somewhat longer than that for $43SNO^{-}$* ($\tau_{rcb} = 4.6$ vs 2.8 ps) and its decay time is slightly shorter ($\tau_{dcb} = 19$ vs 25 ps). The transient absorption spectra of 34SNOH differ from those of 44SNOH in that they display no emissive components and a single absorption band that decays with a lifetime of 12 ps with little change in band shape. They more nearly resemble the transient spectra of 44SNOMe, which does not undergo ESPT. On this basis, the transient spectra of 34SNOH are assigned to the singlet state 34SNOH* rather than to the conjugate base. This assignment is consistent with the exceptionally short fluorescence decay time of 34SNOH* in THF solution (Table 1).

Transient Absorption Spectroscopy of 3SOH and 4SOH. We previously reported that 3SOH* undergoes deprotonation in aqueous solution to yield the fluorescent conjugate base $3SO^{-}$*, but that 4SOH does not.[13,14] We suggested that this difference in excited-state behavior is a consequence of the much longer singlet lifetime for 3SOH vs 4SOH. The longer singlet lifetime of 3SOH is a function of a larger barrier for singlet state C═C torsion, a result of the "meta effect".[24] We were unable to determine the lifetime of 3SOH* by means of time-resolved fluorescence using an apparatus with an instrument response function of 50 ps, placing a lower bound on the value of $k_H < 2 \times 10^{10}$ s^{-1}, similar to the value for 1-naphthol.[2]

The transient spectra for 3SOH (Figure 7a) are similar to those for 43SNOH (Figure 5b). Formation of the 530 nm transient occurs with an instrument-limited rise time. The red edge of this band has a decay time of 2.0 ps, attributed to vibrational cooling of the FC singlet state, which is accompanied by a shift in the absorption maximum to 480 nm. The decay of the 480 nm band is best fit by a dual exponential with decay times of 29 and 490 ps. The blue edge of the absorption band has a rise time of 37 ps, similar to the short-lived component of the 480

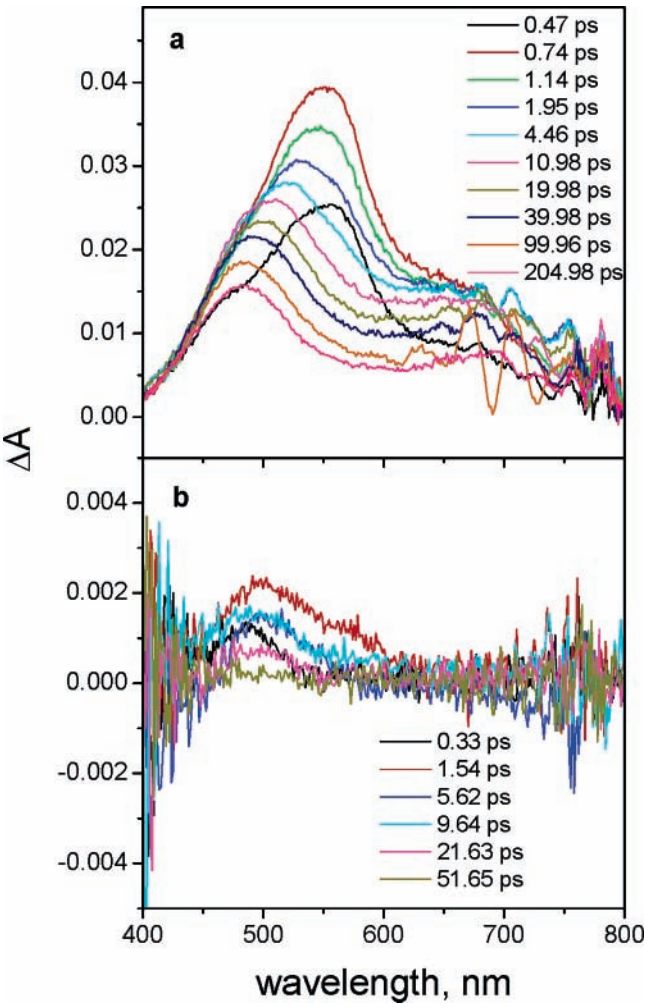

Figure 7. Transient absorption spectra for (a) 3SOH and (b) 4SOH in MW solution.

nm decay, both of which are attributed to ESPT with formation of $3SOH^{-}$*. The long-lived 480 nm decay component is similar to the major (500 ps) component of the fluorescence decay of $3SOH^{-}$* determined in aqueous base.[14]

The 500 nm transient of 4SOH (Figure 7b) has an instrument-limited rise time and a decay time of 17 ps. The signal amplitude is much weaker than that for 44SNOH. The low signal amplitude and short decay time can be attributed to rapid decay of 4SOH* and/or $4SO^{-}$* via C═C torsion. The assignment of the 500 nm transient to 4SOH* rather than to its conjugate base is consistent with the short fluorescence decay time of 4SOH in THF solution (ca. 30 ps) and its low fluorescence quantum yield in aqueous solution.[14] The dynamics of the formation and decay of singlet 4SOH, 3SOH, and 3SO− are reported in Table 3.

Dynamics of Conjugate Base Formation and Decay. The 1.7 ps rise time for the 420 nm transient attributed to formation of $44SNO^{-}$* from 44SNOH* is slightly faster than the value of 2.2 ps recently reported by Poizat et al.[11] for the 6-hydroxyquinolinium ion in acidic solution. Pines et al.[5] have reported that deprotonation of singlet 5-cyano-1-naphthol in water occurs with lifetimes of ca. 8 and 10 ps in water and MW (1/1 by volume), respectively. They suggest that the time scale for solvent-mediated proton-transfer in water can be bracketed by the Debye and Onsager relaxation times ($\tau_D \sim 8$ ps and $\tau_L \sim 0.5$ ps, respectively). Our values of τ_{rcb} for 44SNOH (Table 3) lies in the middle of this range.

Pines et al.[5] have investigated the effects of MW solvent composition and deuteration upon the dynamics of ESPT for the super photoacid 5-cyano-1-naphthol. They report that the dissociation lifetime increases with increasing methanol content from ca. 10 ps in 50% methanol to ca. 25 ps in 90% methanol and 390 ps in pure methanol. A similar decrease in the rate of ESPT for 44SNOH would account for our failure to observe the formation of $44SNO^{-}$* in either 90% methanol or pure methanol. The 14 ps singlet decay time of 44SNOH in methanol (Table 1) presumably is too fast to permit competing ESPT to occur. Pines et al.[5] report that the isotope effect for ESPT depends on the solvent composition, increasing from ca. 1.5 in water to 2.5 in methanol. The rise times for $44SNO^{-}$* formation in MW vs deuterated MW (Table 3) provide an isotope effect of ca. 1.3 ± 0.2. This value is similar to the isotope effect for the dielectric response of water.[5]

Agmon et al.[35] have investigated the photoacidity of cyanonaphthols using AM1 calculations to determine the Mulliken charges on oxygen and the ring carbons of the acid and its conjugate base. They find that the strongest acids have the lowest charge densities on oxygen in the singlet state of the conjugate base. The exceptionally high kinetic acidity of 44SNOH can similarly be attributed to charge delocalization in the relaxed singlet state of its conjugate base, which can be described as a phenoxide→benzonitrile CT state (Figure 2b).

The 30 ps decay time for the conjugate base $44SNO^{-}$* is significantly faster than that for $3SO^{-}$ (Table 4) or for the conjugate base of the super photoacid 5-cyano-1-naphthol ($\tau_{cb} = 110$ ps).[5] It seems unlikely that the short decay time of $44SNO^{-}$* is a consequence of quenching by reprotonation, which would require rates that are much faster than those reported for weaker photoacids. Huppert et al.[36] have observed small positive solvent isotope effects for geminate reprotonation of the conjugate base of several cyano-substituted 2-naphthols in H_2O vs D_2O. Reprotonation can occur via both reversible and irreversible mechanisms.[37] We observe a small positive isotope effect for the decay of SNO^{-}* transient absorption; however, a small negative isotope effect is obtained from the rise time for its fluorescence (Table 4). Thus the decay kinetics provide ambiguous evidence for quenching by reprotonation. The rapid bleaching of 44SNOH absorbance upon irradiation (Figure 3) suggests that $44SNO^{-}$* undergoes rapid C═C torsion, as is the case for the singlet state of 4-aminostilbene.[24]

The excited-state behavior of 44SNOH in MW is summarized in Scheme 1. The low fluorescence quantum yield for 44SNOH* indicates that its lifetime is determined by the rate constant for transfer of a proton to water (k_H). Similarly, the low fluorescence quantum yield for $44SNO^{-}$* indicates that its lifetime is determined by the rate constant for nonradiative decay via internal conversion or C═C torsion (k_{ic} and k_t, respectively). Rapid and efficient isomerization of 44SNOH in MW (Figure 3) is consistent with C═C torsion as the dominant decay pathway for $44SNO^{-}$*. The 30 ps lifetime for $44SNO^{-}$* provides a value of $k_t \sim 3 \times 10^{10}$ s^{-1}. The efficient isomerization and 33 ps lifetime for 44SNOMe* suggests that deprotonation has little effect on the barrier for C═C torsion.

The other 4-hydroxystilbenes, 4SOH and 34SNOH, also form short-lived 480 nm transients in MW (17 and 12 ps, respectively) but fail to display emission from their conjugate bases in either their steady state or transient spectra. We previously attributed the absence of steady-state emission from $4SO^{-}$* to the failure of 4SOH* ESPT to compete with C═C torsion.[13,14] However, it is also possible that 4SOH* does in fact undergo ESPT, but that $4SO^{-}$* undergoes C═C torsion more rapidly than it is formed, thus precluding the observation of either transient absorption or fluorescence from $4SO^{-}$*.

The dynamics conjugate base formation and decay for 43SNOH are strikingly similar to those for 44SNOH (Table 3). The weaker fluorescence from 43SNOH* in MW and 43SNO$^-$* in MW−KOH when compared to 44SNOH* and 44SNO$^-$* is a consequence of lower fluorescence rate constants for the 3- vs 4-hydroxystilbenes.

Unlike 44SNOH, 43SNOH does not undergo rapid photoisomerization in MW (Figure 3). Thus the dominant decay pathway for 43SNO$^-$* must be internal conversion to its ground state (Scheme 1) with a rate constant $k_{ic} \sim 4 \times 10^{10}$ s^{-1}. Rapid internal conversion has been reported for a number of push−pull substituted stilbenes.[25] The transient dynamics for 33SNOH are similar to those for 43SNOH, suggesting similar rate constants for the formation and nonradiative decay of its conjugate base.

The rate constants for both the formation and decay of 3SO$^-$* are appreciably slower than those for 43- and 33SNO$^-$* (Table 3), permitting the observation of fluorescence from both 3SOH* and 3SO$^-$* in aqueous solution. The observation of efficient photoisomerization for 3SOH in MW (Figure 3) indicates that 3SO$^-$* decays predominantly via C═C torsion rather than internal conversion (Scheme 1, $k_t > k_{ic}$). The relatively long lifetime of 3SO$^-$* requires that torsion be relatively slow ($k_t < 2 \times 10^9$ s^{-1}) when compared to the rate constant for internal conversion of 43SNO$^-$*.

Concluding Remarks

The use of fs transient absorption spectroscopy has permitted investigation of the dynamics of proton transfer for the hydroxystilbenes and their cyano derivatives in methanol−water mixed solvents. Assignment of their transient absorption spectra is supported by the use of models for the singlet and its conjugate base. The short decay times of these photoacids and weak fluorescence of their conjugate bases renders impractical the study of their dynamics by transient fluorescence. The ESPT rates for the cyanohydroxystilbenes 43SNOH and 44SNOH are comparable to the fastest reported to date[11] and the solvent deuterium isotope effect the smallest reported to date for a photoacid in water or methanol−water.[5] Both the rate constants for ESPT and the isotope effect approach the theoretical limits for water-mediated proton transfer.

The initial objective of our studies of the hydroxystilbenes was to determine the generality of the "meta effect" for substituted stilbenes. Amine, methoxy, and hydroxy substituents, all of which are strongly mesomeric, are found to markedly increase the stilbene lifetime when located in the meta, but not in the para position.[13,14,24] This manifestation of the generalized "meta effect", as initially formulated by Zimmerman,[38] is attributed to selective stabilization of the planar stilbene singlet state vs the twisted singlet, resulting in an enhanced barrier for C═C torsion. The present results establish that the behavior of both the cyanohydroxystilbenes and their conjugate bases are subject to the meta effect. In nonaqueous solution the singlet states of 43SNOH and 33SNOH have relatively long singlet lifetimes and high fluorescence quantum yields, indicative of high C═C torsional barriers; whereas both 44SNOH and 34SNOH have short singlet lifetimes and low fluorescence quantum yields, indicative of low C═C torsional barriers. The excited conjugate base 43SNO$^-$* decays via internal conversion, whereas 44SNO$^-$* decays via C═C torsion. Thus C═C torsional barriers for the conjugate bases parallel those of the neutrals. As previously observed in our studies of the cyanoaminostilbenes,[25] it is the position of the hydroxy and not the cyano substituent that determines the C═C barrier and thus the excited-state behavior of the cyanohydroxystilbenes.

Acknowledgment. Funding for this project was provided by grants from the National Science Foundation (CHE-0100596 and CHE-0400663).

Supporting Information Available: ZINDO-calculated singlet states and Lippert−Mataga Plots for the cyanohydroxystilbenes and transient absorption data for the 3-cyanohydroxystilbenes. This material is available free of charge via the Internet at http://pubs.acs.org.

References and Notes

(1) (a) Martynov, I. Y.; Demyashkevich, A. B.; Uzhinov, B. M.; Kuz'min, M. G. *Russ. Chem. Rev. Usp. Khim.* **1977**, *46*, 1−15. (b) Arnaut, L. G.; Formosinho, S. J. *J. Photochem. Photobiol., A* **1993**, *75*, 1−20. (c) Tolbert, L. M.; Solntsev, K. M. *Acc. Chem. Res.* **2002**, *35*, 19−27. (d) Agmon, N. *J. Phys. Chem. A* **2005**, *109*, 13−35.

(2) Webb, S. P.; Yeh, S. W.; Philips, L. A.; Tolbert, M. A.; Clark, J. H. *J. Am. Chem. Soc.* **1984**, *106*, 7286−7288.

(3) (a) Webb, S. P.; Philips, L. A.; Yeh, S. W.; Tolbert, L. M.; Clark, J. H. *J. Phys. Chem.* **1986**, *90*, 5154−5164.

(4) Tolbert, L. M.; Haubrich, J. E. *J. Am. Chem. Soc.* **1990**, *112*, 8163−8165. (b) Tolbert, L. M.; Haubrich, J. E. *J. Am. Chem. Soc.* **1994**, *116*, 10593−10600.

(5) Pines, E.; Pines, D.; Barak, T.; Magnes, B.-Z.; Tolbert, L. M.; Haubrich, J. E. *Ber. Bunsen-Ges. Phys. Chem.* **1998**, *102*, 511−517.

(6) Förster, T. *Z. Elektrochem.* **1950**, *54*, 531−535.

(7) Weller, A. *Prog. React. Kinet.* **1961**, *1*, 187−214.

(8) Tolbert, L. M. *Acc. Chem. Res.* **1986**, *19*, 268−273.

(9) (a) Genosar, L.; Cohen, B.; Huppert, D. *J. Phys. Chem. A* **2000**, *104*, 6689−6698. (b) Rini, M.; Magnes, B.-Z.; Pines, E.; Nibbering, E. T. J. *Science* **2003**, *301*, 349−352.

(10) Cohen, B.; Leiderman, P.; Huppert, D. *J. Lumin.* **2003**, *102*−*103*, 682−687.

(11) Poizat, O.; Bardez, E.; Buntinx, G.; Alain, V. *J. Phys. Chem. A* **2004**, *108*, 1873−1880.

(12) Solntsev, K. M.; Sullivan, E. N.; Tolbert, L. M.; Ashkenazi, S.; Leiderman, P.; Huppert, D. *J. Am. Chem. Soc.* **2004**, *126*, 12701−12708.

(13) Lewis, F. D.; Crompton, E. M. *J. Am. Chem. Soc.* **2003**, *125*, 4044−4045.

(14) Crompton, E. M.; Lewis, F. D. *Photochem. Photobiol. Sci.* **2004**, *3*, 660−668.

(15) Lee, B. H.; Marvel, C. S. *J. Polym. Sci., Polym. Chem. Ed.* **1982**, *20*, 393−399.

(16) McOmie, J. F. W.; Watts, M. L.; West, D. E. *Tetrahedron* **1968**, *24*, 2289−2292.

(17) Weigel, W.; Rettig, W.; Dekhtyar, M.; Modrakowski, C.; Beinhoff, M.; Schlueter, A. D. *J. Phys. Chem. A* **2003**, *107*, 5941−5947.

(18) *CAChe*, 4.4; Fujitsu Limited: Chiba, Japan,

(19) Rybtchinski, B.; Sinks, L.; Wasielewski, M. R. *J. Phys. Chem. A* **2004**, *108*, 7497−7505.

(20) Lukas, A. S.; Miller, S. E.; Wasielewski, M. R. *J. Phys. Chem. B* **2000**, *104*, 931−940.

(21) Giaimo, J. M.; Gusev, A. V.; Wasielewski, M. R. *J. Am. Chem. Soc.* **2002**, *124*, 8530−8531.

(22) Data provided as Supporting Information.

(23) Zerner, M. C.; Loew, G. H.; Kirchner, R. F.; Mueller-Westerhoff, U. T. *J. Am. Chem. Soc.* **1980**, *102*, 589−599.

(24) Lewis, F. D.; Kalgutkar, R. S.; Yang, J.-S. *J. Am. Chem. Soc.* **1999**, *121*, 12045−12053.

(25) Lewis, F. D.; Weigel, W. *J. Phys. Chem. A* **2000**, *104*, 8146−8153.

(26) Solntsev, K. M.; Huppert, D.; Agmon, N. *J. Phys. Chem. A* **1998**, *102*, 9599−9606. Solntsev, K. M.; Huppert, D.; Agmon, N. *J. Phys. Chem. A* **1999**, *103*, 6984−6997.

(27) Clower, C.; Solntsev, K. M.; Kowalik, J.; Tolbert, L. M.; Huppert, D. *J. Phys. Chem. A* **2002**, *106*, 3114−3122.

(28) Murohoshi, T.; Kaneda, K.; Ikegami, M.; Arai, T. *Photochem. Photobiol. Sci.* **2003**, *2*, 1247−1249.

(29) Waldeck, D. H. *Chem. Rev.* **1991**, *91*, 415−436.

(30) Hochstrasser, R. M. *Pure Appl. Chem.* **1980**, *1980*, 2683−2691.

(31) Iwata, K.; Hamaguchi, H. *Chem. Phys. Lett.* **1992**, *196*, 462−468. Schultz, S. L.; Qian, J.; Jean, J. M. *J. Phys. Chem. A* **1997**, *101*, 1000−1006.

(32) Pines, D.; Pines, E.; Rettig, W. *J. Phys. Chem. A* **2003**, *107*, 236−242.

(33) Lewis, F. D.; Wu, T.; Liu, X.; Letsinger, R. L.; Greenfield, S. R.; Miller, S. E.; Wasielewski, M. R. *J. Am. Chem. Soc.* **2000**, *122*, 2889−2902.

(34) Papper, V.; Pines, D.; Likhtenshtein, G.; Pines, E. *J. Photochem. Photobiol. A.* **1997**, *111*, 87−96.

(35) Agmon, N.; Rettig, W.; Groth, C. *J. Am. Chem. Soc*. **2002**, *124*, 1089−1096.
(36) Huppert, D.; Tolbert, L. M.; Linares-Samaniego, S. *J. Phys. Chem. A* **1997**, *101*, 4602−4605.
(37) (a) Pines, E.; Huppert, D.; Agmon, N. *J. Chem. Phys.* **1988**, *88*, 5620−5630. (b) Solntsev, K. M.; Agmon, N. *Chem. Phys. Lett*. **2000**, *320*, 262−268. (c) Solntsev, K. M.; Huppert, D.; Agmon, N.; Tolbert, L. M. *J. Phys. Chem. A* **2000**, *104*, 4658−4669. (d) Cohen, B.; Huppert, D. *J. Phys. Chem. A* **2001**, *105*, 2980−2988.
(38) (a) Zimmerman, H. E. *J. Am. Chem. Soc.* **1995**, *117*, 8988−8991. (b) Zimmerman, H. E. *J. Phys. Chem. A* **1998**, *102*, 5616−5621, and references therein.